

# Shattering during Surface-Induced Dissociation: An Examination of Peptide Size and Structure

George L. Barnes<sup>a,\*</sup>, Amanda Shlaferman<sup>a</sup>, Monica Strain<sup>a</sup>

*<sup>a</sup>Department of Chemistry and Biochemistry  
Siena College  
515 Loudon Road  
Loudonville, NY 12211*

---

## Abstract

We present the results of direct dynamics simulations of surface-induced dissociation for  $A_nK$ ,  $KA_n$  ( $n = 1, 3, \text{ and } 5$ ),  $AcA_7K$ , and  $AcKA_7$  for collisions with a fluorinated self-assembled monolayer surface. Our focus is on elucidating shattering fragmentation events, which takes place in coincidence with the collision event and frequently occurs in a charge remote fashion. Shattering events typically generate a large number of fragmentation products, and hence, are not easily understood through chemical intuition. Our simulations show distinct differences between the  $A_nK/AcA_7K$  and  $KA_n/AcKA_7$  series of peptides, with the former being more reactive, while the latter is more selective regarding the type of bond that will break. In addition, we examine the possible backbone rearrangements seen as well as sidechain fragmentation.

*Keywords:* Tandem Mass Spectrometry, Direct Dynamics Simulations, Surface-Induced Dissociation, Shattering Fragmentation

---

## 1. Introduction

Surface-induced dissociation (SID) is a well-studied analytical technique that has frequently been used to study the fragmentation of biological ions [1, 2]. Surfaces such as diamond as well as organic self-assembled monolayer (SAM) surfaces are commonly used in this technique, and protonated peptides have been a particular focus of SID studies [3, 4]. During SID, an ion with a known mass to charge ratio is imparted a precise translational energy and directed towards a surface with a given incidence angle. The resulting collision allows for translational to internal energy transfer with fragmentation occurring when a sufficient amount of energy is deposited into individual bonds. Hence, fragmentation can take a significant amount of time as intramolecular vibrational relaxation (IVR) redistributes the transferred energy throughout the molecule. However, it has also been seen computationally, as well as experimentally, that fragmentation can occur in coincidence with the collision event. Such fragmentation events have been termed “shattering.”[3, 5–13]

Shattering is known to produce an incredibly large number of different reactive products within experiments [1] and simulations [13] of protonated peptides. Unlike statistical fragmentation of peptide ions, in which the IVR process is complete and fragmentation is often driven by proton motion (i.e. the mobile proton model [14]), it is common for shattering fragmentation to occur in a charge remote fashion. One of the incredibly nice features of proton driven fragmentation is the intuitive picture that is provided, namely that a proton is mobilized and migrates to a thermodynamically less stable site, which in turn weakens a covalent bond and makes it more likely to cleave. There is no equivalent intuitive picture available for shattering fragmentation, which is in part due to the somewhat overwhelming number of different fragmentation products possible.

There has been a significant computational focus on shattering in  $gly_n-H^+$  + surface systems [9, 11–13] with  $n=1, 2$  and 8. This work provides greater insight into shattering by presenting a direct dynamics study of a complementary series of protonated peptides, namely  $A_nK$  and  $KA_n$  ( $n = 1, 3, 5$ ) as well as  $AcA_7K$  and  $AcKA_7$  colliding with a fluorinated SAM (FSAM) surface.  $AcA_7K$  and  $AcKA_7$  were the subject of a previous work focused

---

\*Corresponding author

Email address: gbarnes@siena.edu (George L. Barnes)

on soft-landing [15], but are also clearly complementary to the present study. This choice of protonated peptides probes very small dipeptides up to octapeptides, and allows for a limited examination of globular vs alpha-helical secondary structure while also increasing the chemical diversity of systems explored by direct dynamics. In addition, we seek to provide insight into the types of bonds that are most likely to be cleaved during a shattering event rather than focusing on individual products for a specific system. In order to accomplish this, we will identify the final product ion based on the bond cleavage sites as defined using the established nomenclature for protonated peptide ion products [16]. Moreover, we seek to determine if there is either a size or structural correlation with the types of bonds cleaved.

## 2. Method

Below we describe our method for obtaining the initial structures for each species as well as for performing the direct dynamics simulations. The work can also be viewed as an extension of that of Frederickson *et al.* [15], which focused on soft landing while this work focuses on shattering.

### 2.1. Initial Structures

Structures are needed for eight different species, namely  $A_nK$  and  $KA_n$  with  $n = 1, 3, \text{ and } 5$  as well as  $AcA_7K$  and  $AcKA_7$ . The latter two structures are taken from Frederickson *et al.* As described in that work, Jarrold and co-workers found that  $AcA_7K$  is the shortest, stable alpha-helical peptide known, while  $AcKA_7$  has a globular form [17]. In this work, we were able to form an alpha-helical structure for  $A_5K$  that was stable for our short-time, gas phase simulations. All other structures are globular. The  $A_5K$  structure was obtained via Avogadro [18] and then optimized using the RM1 semi-empirical method [19]. RM1 was selected since it was used in the soft-landing work of Frederickson *et al.* as well as numerous other direct dynamics simulations of protonated peptides [20–26].

The structure for all other species were obtained by obtaining an initial structure via Avogadro and reoptimizing it via GROMACS [27] with the OPLS force field followed by a 100 ps equilibration at 300K. A simulated annealing procedure was then applied using 20 heat-cool cycles in which the temperature was ramped to 1000 K over 100 ps and then cooled to 0 K over an additional 100 ps. All of the 0 K structures were optimized at the RM1 level as implemented in Mopac2016 [28]. The lowest energy conformation was selected from these structures as

the initial starting point for the direct dynamics simulations. All structures are shown in Appendix A. These species show a diverse range of conformations, and the  $A_nK$  and  $KA_n$  series have distinct differences.  $AK$  and  $KA$  both exhibit hydrogen bonding between the protonated N of the sidechain and the N-terminus. However,  $KA$  also shows a close proximity to the C-terminus and has additional stabilization. This trend continues to  $A_3K$  and  $KA_3$ .  $A_3K$  is hydrogen bound to a carbonyl along the backbone, whereas  $KA_3$  retains the sidechain to N-terminus hydrogen bond as well as being in close proximity to the C-terminus.  $A_5K$  and  $AcA_7K$  are both alpha helical, and hence, are more elongated whereas  $KA_5$  and  $AcKA_7$  have formed a “pocket” of carbonyl groups that are associated with the side chain nitrogen group. Energetically speaking, the alpha helical structures are higher in energy than the those of  $KA_5$  and  $AcKA_7$ .

### 2.2. Direct Dynamics Simulations

Our approach to performing direct dynamics simulations of collision systems relevant to mass spectrometry has recently been detailed in three review articles [29–31], and hence, we shall only provide an outline of the approach here. Several of the original works on the specific topic of protonated peptides colliding with organic self-assembled monolayers [9, 32–34] would also provide additional technical detail.

We begin by writing the potential energy as a sum of three components, namely

$$V = V_{peptide} + V_{SAM} + V_{peptide-SAM} \quad (1)$$

where  $V_{SAM}$  is the intramolecular, molecular mechanical (MM) force field for FSAMs and  $V_{peptide-SAM}$  is the most recent MM force field for the interaction between a protonated peptide and the SAM surface. This force field, developed by Hase and co-workers, is specifically designed for modeling soft landing [35, 36]. However, it also performs well at higher collision energies, such as those considered here. The peptide potential,  $V_{peptide}$ , is treated using the RM1 semi-empirical method for the reasons described in the previous section.

The peptide is initially placed 40 Å above a 9x9 octanethiol FSAM surface with a random orientation. Initial positions and velocities were randomly selected for both the surface and the peptide using a velocity re-scaling routine such that each was given an initial temperature of 300 K. Separate MD simulations were performed for the peptide and the surface with velocity re-scaling occurring every 30 time steps. This approach was successfully used by Frederickson *et al.*[15]. Lastly, a relative collision energy

of 100 eV with a normal incidence angle was imparted to the peptide. One thousand trajectories were calculated for each species.

Hamilton’s equations of motion were integrated using a 6<sup>th</sup> order symplectic integration scheme [37], making use of a one femtosecond step size with output written every 50 femtoseconds. Trajectories were stopped after five picoseconds of simulation time. Conservation of energy was continually checked during the simulations. If a large jump in energy conservation was seen for any given step, it was rejected and the time step was re-integrated using five 0.2 fs time steps. Assuming energy was well conserved following this, the normal time step was reinstated. This precaution was important to implement as a fairly large number of trajectories ( $\sim 5\%$ ) were exhibiting poor conservation of energy. It was determined that the majority of the error was accumulated in a single integration step. This is perhaps not surprising as we are investigating fairly high energy systems undergoing abrupt changes in momentum. All simulations were performed using an in-house simulation code coupled to Mopac2012 [38].

### 3. Results and Discussion

We begin our analysis by examining the overall reactivity for the species, as shown in Figure 1. There are three immediate trends that are observed on this time scale: 1) Reactivity decreases with peptide size, 2) shattering both decreases with system size, but also becomes relatively more important, and 3) the  $A_nK$  series (including  $AcA_7K$ ) is more reactive than the  $KA_n$  series (including  $AcKA_7$ ). There is an important realization to make regarding the fractions shown in Figure 1, namely that the fraction of shattering trajectories cannot change whereas the fraction of non-shattering trajectories depends on the overall simulation time. Hence, the observed difference between  $AK$  and  $KA$  in overall reactivity will not necessarily prove to hold in the long time limit as the dynamics of  $KA$  are likely slower due to the extra stabilization present. This trend continues throughout the  $A_nK$  and  $KA_n$  series, with the latter having reduced overall reactivity due to the favorable energetics for that family of structures.

The shattering fraction is fixed and cannot change with a longer simulation time. It is interesting to note that the shattering fraction depends on the system size and decreases by more than a factor of four, moving from the smallest to the largest system size. At first, this observation may be surprising as one could argue that shattering should not strongly depend on size as it is the result of

a strong local force, i.e. impulsive impact with the surface. We believe that the reason the system size clearly does have a large effect on the shattering fraction is that the energy transfer is distributed among more parts of the molecule. It is known that the percentage of translational to internal energy transfer does not depend on system size, and hence, the same percentage of the 100 eV collision energy is being put into, for example, both  $AK$  and  $AcA_7K$ . However, the number of atoms - and therefore chemical groups - that come into close contact with the surface is dramatically different. With a greater number of groups accepting energy, there are more bonds within which to distribute the same amount of energy. This makes shattering less likely for a larger system. This also suggests that there could be a strong orientational effect on shattering, though we have not examined that here.

The question of the role of secondary structure is not conclusively answered from data in Figure 1. Although it is seen, for example, that  $A_5K$  (alpha-helical) has a larger shattering fraction than  $KA_5$  (globular) the same is true for  $A_3K$  vs  $KA_3$ , which are both globular in nature. Therefore, the primary sequence itself appears to be more important. However, this may also be an artifact of these two particular series of peptides, namely that  $KA_n$  naturally has more energetically favorable structures than  $A_nK$ . This would also be in line with the cluster-surface shattering work, which determined that the fragment distribution is related to the species stability [5].

To continue our examination of shattering, we will use the standard nomenclature scheme [16] as depicted in Figure 2. Our direct dynamics simulations automatically track connectivity. This information can be used to determine the backbone as well as sidechain cleavage sites. To ease the discussion, we will now turn our attention to three classes of shattering products: so called “simple shattering products” (which we define below), backbone rearrangements, and side chain fragmentation.

#### 3.1. Simple Shattering Products

Simple shattering products are those whose final ion contain a partially intact backbone that could have resulted from a single backbone cleavage event. This does not mean that the trajectory in fact only had a single backbone cleavage, but merely that the charged portion of the peptide could have resulted from a single backbone cleavage. For example, if the final product ion is an  $a1$  ion, it is entirely possible for the  $b1$  site to have also broken, resulting in the formation of  $CO$  as well as the remainder of the neutral peptide along with the  $a1$  ion. Hence, the ion from a simple shattering product corresponds to the infor-

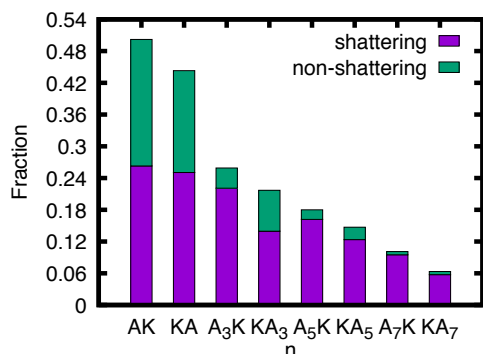


Figure 1: The fraction of reactive trajectories broken down into shattering and non-shattering as a function of species. Note that A<sub>7</sub>K and KA<sub>7</sub> are in fact acetylated. See Appendix A to see the conformation of each.

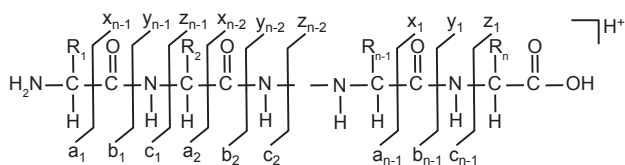


Figure 2: Definition of ion types.

mation directly provided by an experimental mass spectrum. Figure 3 examines the location of the backbone cleavage event as a function of ion type irrespective to location along the backbone. Meaning both an a1 and a4 would both contribute to the fraction relative to all shattering events for the a-type fragmentation. It is important to note that this figure does not suggest that all of the ions generated would have the  $m/z$  value associated with an a-ion because there could be other rearrangements that take place, such as a methyl shift. Rather this figure provides information regarding the most likely type of bond to break within the backbone along with which side of the peptide is charged following the bond cleavage. The fractions do not add up to 1 in this figure because not all shattering products are simple shattering products.

Figure 3 shows clear differences between the A<sub>n</sub>K and KA<sub>n</sub> series. In the KA<sub>n</sub> series, the a-type ion is the dominant pathway for all species. In the A<sub>n</sub>K series, both the a- and x-type ions are common, with the x-type dominating at large system size and the a-type dominating at small system size. It is also possible to examine the most probable bond cleavage sites individually, which is shown in Figure 4. In this figure, the heavy atoms of each species are shown along with lines that designate

the backbone cleavage location. Red lines denote that the charge is towards the N-terminus, whereas blue lines denote the charge is towards the C-terminus. The thickness of the line provides the relative importance of that cleavage site. Figure 4 shows that although the a-type ion is dominant for the KA<sub>n</sub> series, the cleavage events are distributed among several possible a-sites. For KA<sub>n</sub> with  $n=1, 3$  and  $5$ , the a1 site is the most likely cleavage point. For example, in the KA<sub>3</sub> system, the a1 site is nearly twice as likely as either the a2 or the a3 site. For AcKA<sub>7</sub>, a4 and a7 sites are the most likely cleavage locations, with the a4 site being a little less than twice as likely than the a1 site. That said, there are a significantly smaller number of shattering events for this system (see Figure 1).

Turning our attention to the A<sub>n</sub>K series, Figure 4 highlights the shift in preference between a-type and b-type cleavage events with system size. The a1 site is the dominant cleavage location for AK, whereas the a1 site is in competition with the x3 site as well as the x2 and a2 sites for A<sub>3</sub>K. Both A<sub>5</sub>K and AcA<sub>7</sub>K are alpha helical, and here, we see the x-type cleavage events becoming dominant. Once again, we see a distribution of sites in the middle of the sequence with x4 and x5 being the most likely and roughly twice as likely as the x1 site. The A<sub>n</sub>K series also retains some a-type cleavage events, with a4, for example, being a little less than half as likely as x4. This is a difference between the two series - A<sub>n</sub>K has some competition between x-type and a-type throughout whereas the KA<sub>n</sub> series is dominated by a-type.

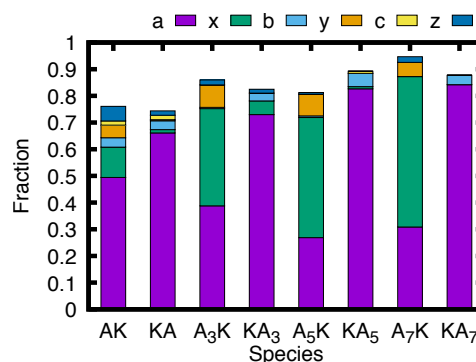


Figure 3: The fraction of ion sites for shattering fragmentation events that results from a single cleavage along the backbone. We note that we are using the ion nomenclature to identify the bond cleavage sites and the side of the peptide retaining the charge - not the final ion  $m/z$ , since additional rearrangements are possible.

### 3.2. Backbone Rearrangements

As described above, Figure 3 does not have fractions that add up to 1 because there are fragmentation events



ture of shattering reaction dynamics.

### 3.3. Sidechain Fragmentation

Another type of shattering event that is not captured in Figure 3 is fragmentation of the side chain alone. This occurs through two major pathways: 1) loss of  $\text{NH}_3$  from the lysine, and 2) complete loss of the charged side chain. In the former, the system is stabilized by forming a cyclic structure, whereas in the latter the proton transfers back to the backbone.

## 4. Summary

Our simulation results show that there is a strong system size dependence on the fraction of shattering trajectories, with small systems having a greater likelihood of shattering than large systems for the same collision energy. This result is suggestive as to why few experiments have reported shattering products for protonated peptides, namely that most experimental systems are of sufficient size that it is plausible for shattering fragmentation to be a minor producer of final products.

Differences are also observed between the  $\text{A}_n\text{K}$  and  $\text{KA}_n$  family of peptides, with  $\text{A}_n\text{K}$  being more reactive than  $\text{KA}_n$ . However,  $\text{KA}_n$  is more selective in the type of shattering fragmentation that is observed, with b-ions being prevalent for all system sizes. In contrast,  $\text{A}_n\text{K}$  shows a preference for a-ions for small systems and b-ions for large system sizes. We were not able to make conclusive statements regarding the importance of secondary structure. However, our data does support that either primary structure or overall energetics is an important driver of the shattering fraction.

The majority of shattering fragments, at the end of our short time simulations, can be described as simple shattering products meaning that the final charged product has a sequence of backbone atoms that could result from cleavage at a single backbone site. More complicated products are also observed that result from backbone rearrangements, although these are not as common as the simple products. Sidechain fragmentation alone is also possible, and in these systems is exclusive to the lysine amino acid group.

## 5. ACKNOWLEDGEMENTS

GLB, AS, and MS gratefully acknowledge support from the National Science Foundation under grant number 1763652. GLB dedicates this work to Prof. William L. Hase, his post-doctoral advisor, who passed away on Monday, March 23, 2020.

## 6. Appendix A. Supplementary data

Supplementary data to this article can be found online.

## References

- [1] J. Laskin, Ion-surface collisions in mass spectrometry: Where analytical chemistry meets surface science, *Int. J. Mass Spectrom.* 377 (2015) 188–200. doi:10.1016/j.ijms.2014.07.004.
- [2] V. H. Wysocki, K. E. Joyce, C. M. Jones, R. L. Beardsley, Surface-induced dissociation of small molecules, peptides, and non-covalent protein complexes., *J. Am. Soc. Mass Spectrom.* 19 (2) (2008) 190–208. doi:10.1016/j.jasms.2007.11.005.
- [3] J. Laskin, T. H. Bailey, J. H. Futrell, Shattering of Peptide Ions on Self-Assembled Monolayer Surfaces., *J. Am. Chem. Soc.* 125 (6) (2003) 1625–1632. doi:10.1021/ja027915t.
- [4] J. Laskin, J. H. Futrell, Energy Transfer in Collisions of Peptide Ions with Surfaces, *J. Chem. Phys.* 119 (6) (2003) 3413–3420. doi:10.1063/1.1589739.
- [5] T. Raz, R. D. Levine, On the shattering of clusters by surface impact heating, *J. Chem. Phys.* 105 (18) (1996) 8097–8102. doi:10.1063/1.472663.
- [6] W. Christen, U. Even, Cluster impact chemistry, *J. Phys. Chem. A* 102 (47) (1998) 9420–9426. doi:10.1021/jp981874z.
- [7] W. Christen, U. Even, T. Raz, R. D. Levine, Collisional energy loss in cluster surface impact: Experimental, model, and simulation studies of some relevant factors, *J. Chem. Phys.* 108 (24) (1998) 10262–10273. doi:10.1063/1.476487.
- [8] D. G. Schultz, L. Hanley, Shattering of  $\text{SiMe}_3^+$  during surface-induced dissociation, *J. Chem. Phys.* 109 (24) (1998) 10976. doi:10.1063/1.477737.
- [9] O. Meroueh, W. L. Hase, Effect of Surface Stiffness on the Efficiency of Surface-Induced Dissociation, *Phys. Chem. Chem. Phys.* 3 (12) (2001) 2306–2314. doi:10.1039/b100892g.
- [10] J. Laskin, J. H. Futrell, Surface-Induced Dissociation of Peptide Ions: Kinetics and Dynamics., *J. Am. Soc. Mass Spectrom.* 14 (12) (2003) 1340–1347. doi:10.1016/j.jasms.2003.08.004.
- [11] Y. Wang, W. L. Hase, K. Song, Direct Dynamics Study of N-Protonated Diglycine Surface-Induced Dissociation. Influence of Collision Energy., *J. Am. Soc. Mass Spectrom.* 14 (12) (2003) 1402–1412. doi:10.1016/j.jasms.2003.08.014.
- [12] K. Park, K. Song, W. L. Hase, An ab initio direct dynamics simulation of protonated glycine surface-induced dissociation, *Int. J. Mass Spectrom.* 265 (2-3) (2007) 326–336. doi:10.1016/j.ijms.2007.03.009.
- [13] K. Park, B. Deb, K. Song, W. L. Hase, Importance of Shattering Fragmentation in the Surface-Induced Dissociation of Protonated Octaglycine., *J. Am. Soc. Mass Spectrom.* 20 (6) (2009) 939–948. doi:10.1016/j.jasms.2009.02.028.
- [14] R. Boyd, A. Somogyi, The mobile proton hypothesis in fragmentation of protonated peptides: a perspective., *J. Am. Soc. Mass Spectrom.* 21 (8) (2010) 1275–1278. doi:10.1016/j.jasms.2010.04.017.
- [15] D. Frederickson, M. McDonough, G. L. Barnes, A Computational Comparison of Soft Landing of Alpha-Helical vs Globular Peptides, *J. Phys. Chem. B* 122 (41) (2018) 9549–9554. doi:10.1021/acs.jpcc.8b06232.
- [16] I. A. Papayannopoulos, The interpretation of collision-induced dissociation tandem mass spectra of peptides, *Mass Spectrom. Rev.* 14 (1) (1995) 49–73. doi:10.1002/mas.1280140104.

- [17] R. R. Hudgins, M. F. Jarrold, Helix Formation in Unsolvated Alanine-Based Peptides: Helical Monomers and Helical Dimers, *J. Am. Chem. Soc.* 121 (14) (1999) 3494–3501. doi:10.1021/ja983996a.
- [18] M. D. Hanwell, D. E. Curtis, D. C. Lonie, T. Vandermeersch, E. Zurek, G. R. Hutchison, Avogadro: An Advanced Semantic Chemical Editor, Visualization, and Analysis Platform., *J. Cheminform.* 4 (1) (2012) 17. doi:10.1186/1758-2946-4-17.
- [19] G. B. Rocha, R. O. Freire, A. M. Simas, J. J. P. Stewart, RM1: A Reparameterization of AM1 for H, C, N, O, P, S, F, Cl, Br, and I., *J. Comput. Chem.* 27 (10) (2006) 1101–1111. doi:10.1002/jcc.20425.
- [20] G. L. Barnes, A. Podczewinski, Simulating the Effect of Charge State on Reactive Landing of a Cyclic Tetrapeptide on Chemically Modified Alkylthiolate Self-Assembled Monolayer Surfaces, *J. Phys. Chem. C* 121 (27) (2017) 14628–14635. doi:10.1021/acs.jpcc.7b03478.
- [21] Z. Homayoon, S. Pratihari, E. Dratz, R. Snider, R. Spezia, G. L. Barnes, V. Macaluso, A. Martin Somer, W. L. Hase, Model Simulations of the Thermal Dissociation of the TIK(H<sup>+</sup>)<sub>2</sub> Tripeptide: Mechanisms and Kinetic Parameters, *J. Phys. Chem. A* 120 (42) (2016) 8211–8227. doi:10.1021/acs.jpca.6b05884.
- [22] K. Shaikh, J. Blackwood, G. L. Barnes, The Effect of Protonation Site and Conformation on Surface-Induced Dissociation in a Small, Lysine Containing Peptide, *Chem. Phys. Lett.* 637 (2015) 83–87. doi:10.1016/j.cplett.2015.07.062.
- [23] Z. Gregg, W. Ijaz, S. Jannetti, G. L. Barnes, The Role of Proton Transfer in Surface-Induced Dissociation, *J. Phys. Chem. C* 118 (2014) 22149–22155. doi:10.1021/jp507069x.
- [24] A. Geragotelis, G. L. Barnes, Surface Deposition Resulting from Collisions Between Diglycine and Chemically Modified Alkylthiolate Self-Assembled Monolayer Surfaces, *J. Phys. Chem. C* 117 (25) (2013) 13087–13093. doi:10.1021/jp402424z.
- [25] W. Ijaz, Z. Gregg, G. L. Barnes, Complex Formation during SID and Its Effect on Proton Mobility, *J. Phys. Chem. Lett.* 4 (22) (2013) 3935–3939. doi:10.1021/jz402093q.
- [26] G. L. Barnes, K. Young, L. Yang, W. L. Hase, Fragmentation and Reactivity in Collisions of Protonated Diglycine with Chemically Modified Perfluorinated Alkylthiolate-Self-Assembled Monolayer Surfaces., *J. Chem. Phys.* 134 (9) (2011) 094106. doi:10.1063/1.3558736.
- [27] M. J. Abraham, T. Murtola, R. Schulz, S. Páll, J. C. Smith, B. Hess, E. Lindahl, Gromacs: High performance molecular simulations through multi-level parallelism from laptops to supercomputers, *SoftwareX* 1-2 (2015) 19–25. doi:10.1016/j.softx.2015.06.001.
- [28] J. P. Stewart, Mopac2016 (2016).
- [29] A. Martin Somer, V. Macaluso, G. L. Barnes, L. Yang, S. Pratihari, K. Song, W. L. Hase, R. Spezia, Role of Chemical Dynamics Simulations in Mass Spectrometry Studies of Collision-Induced Dissociation and Collisions of Biological Ions with Organic Surfaces, *J. Am. Soc. Mass Spectrom.* 31 (1) (2020) 2–24. doi:10.1021/jasms.9b00062.
- [30] S. Pratihari, G. L. Barnes, W. L. Hase, S. Pratihara, G. L. Barnes, W. L. Hase, Chemical Dynamics Simulations of Energy Transfer, Surface-Induced Dissociation, Soft-Landing, and Reactive-Landing in Collisions of Protonated Peptide Ions with Organic Surfaces, *Chem. Soc. Rev.* 45 (13) (2015) 3595–3608. doi:10.1039/C5CS00482A.
- [31] S. Pratihari, G. L. Barnes, J. Laskin, W. L. Hase, Dynamics of Protonated Peptide Ion Collisions with Organic Surfaces. Consonance of Simulation and Experiment., *J. Phys. Chem. Lett.* 7 (2016) 3142–3150. doi:10.1021/acs.jpcclett.6b00978.
- [32] G. L. Barnes, W. L. Hase, Energy Transfer, Unfolding, and Fragmentation Dynamics in Collisions of N-Protonated Cctaglycine with an H-SAM Surface., *J. Am. Chem. Soc.* 131 (47) (2009) 17185–17193. doi:10.1021/ja904925p.
- [33] L. Yang, O. A. Mazzyar, U. Lourderaj, J. Wang, M. T. Rodgers, E. Martinez-Núñez, S. V. Addepalli, W. L. Hase, Chemical Dynamics Simulations of Energy Transfer in Collisions of Protonated Peptide Ions with a Perfluorinated Alkylthiol Self-Assembled Monolayer Surface, *J. Phys. Chem. C* 112 (25) (2008) 9377–9386.
- [34] O. Meroueh, W. L. Hase, Dynamics of Energy Transfer in Peptide-Surface Collisions, *J. Am. Chem. Soc.* 124 (7) (2002) 1524–1531. doi:10.1021/ja011987n.
- [35] S. Pratihari, S. C. Kohale, S. A. Vázquez, W. L. Hase, S. A. Va, W. L. Hase, Intermolecular Potential for Binding of Protonated Peptide Ions with Perfluorinated Hydrocarbon Surfaces, *J. Phys. Chem. B* 118 (20) (2014) 5577–5588. doi:10.1021/jp410886s.
- [36] S. Pratihari, N. Kim, S. C. Kohale, W. L. Hase, Mechanistic Details of Energy Transfer and Soft Landing in ala2-H<sup>+</sup> Collisions with a F-SAM Surface, *Phys. Chem. Chem. Phys.* 17 (38) (2015) 24576–24586. doi:10.1039/C5CP03214H.
- [37] C. Schlier, A. Seiter, High-Order Symplectic Integration: An Assessment, *Comput. Phys. Commun.* 130 (1-2) (2000) 176–189. doi:10.1016/S0010-4655(00)00011-4.
- [38] J. P. Stewart, Mopac2012 (2012).